Computational Fluid Dynamics Project

On Incompressible, 3-D, Viscous Laminar Channel Flow

MEMS1071, Applied Fluid Mechanics
Dr. Anne Robertson
Seth Strayer
3/20/19

Contents

List of Parameters

A - cross-sectional area $[m^2]$
D - pipe diameter - $D = 0.01$ [m]
L - pipe length - $L = 0.250$ [m]
μ - viscosity - $\mu = 1 \cdot 10^{-3}$ [kg/(m-s)]
P - pressure $[Pa]$
ρ - density of water - $\rho = 1000$ $[m^3/kg]$
Re - Reynold's Number $[-]$
v - velocity $[m/s]$
Q - volumetric flow rate $[m^3/s]$
x_e - entrance length $[m]$

1 Introduction

In this report, we will perform numerical simulations on incompressible, 3-D, viscous laminar channel flow as shown in Figure 1 using ANSYS Fluent. This flow contains two distinct regions: the developing region and the fully developed region. In the developing region, the boundary layer grows from the channel's inlet and eventually merges together to the centerline of the channel at some point downstream. The distance from the inlet region to the point at which these boundary layers meet is called the *entrance length*, x_e. In this region, there does not exist an exact solution. Past this point, the flow becomes fully developed. In this fully developed region, it is known that the velocity profile and pressure gradient (dp/dx) remain constant, regardless of the streamwise position. The exact solution for this region is known, and its profile is parabolic in nature. In this report, we wish to numerically find the relation of x_e/D to Re_D by addressing the following sub-questions, listed below.

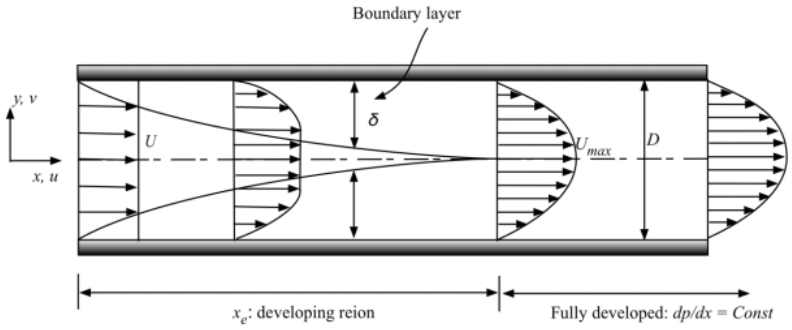

Figure 1: Channel Flow Schematic

- Perform the simulation for $Re_D = 50$. Plot the axial velocity u/U vs. y/D at 10 different axial positions including the developing and fully develped regions.
- Using the numerical results, find dp/dx and Q (volume flow rate) in the fully developed region. Comment on the error between them against the exact solution, given by:

$$Q = \frac{\pi R^4}{8\mu}\frac{dp}{dx} \tag{1}$$

- Find the entrance length, x_e/D for the numerical results.

2 Results

2.1 Velocity Field

In this section, the axial velocity u/U vs. y/D is plotted in 10 different axial positions, as to provide velocity fields in both the developing and fully developed regions. In the fully developed regions, we expect the velocity field to one, remain the same regardless of the streamwise position, and two, to be parabolic in nature. To verify our results, the numerical values obtained from ANSYS Fluent will be plotted against that of the exact solution. In our case, the exact solution is given by flow in a cylindrical pipe driven by a pressure drop. Namely, along the streamwise direction,

$$v = \frac{KR^2}{4\mu}\left(1 - \frac{r^2}{R^2}\right) \tag{2}$$

where K is a constant in the fully developed region, given by the total pressure drop:

$$K = \frac{P_1 - P_2}{L} \tag{3}$$

The total pressure drop was calculated by extracting the numerical data into Microsoft Excel and then calculating the total difference in pressure from the inlet position to the end of the pipe. A plot of the normalized axial velocity vs. the radial position for $Re_D = 50$ is given in Figure 2.

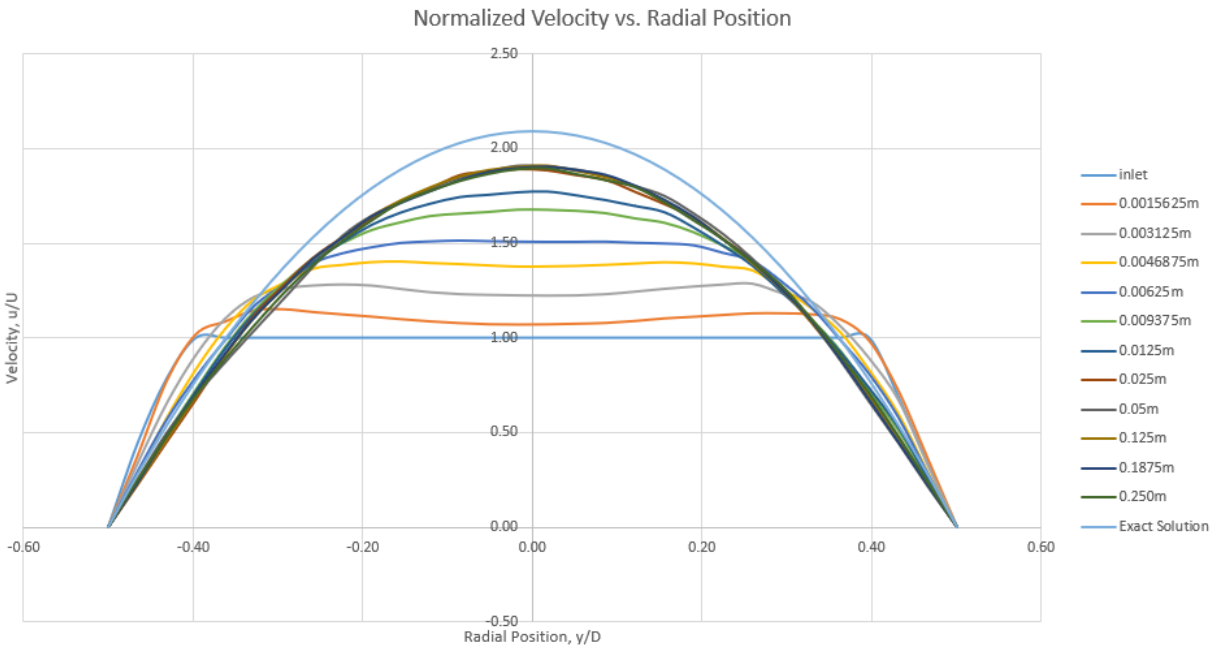

Figure 2: Velocity Fields for $Re_D = 50$

From this plot it is clear that near the inlet where the flow is still developing, the velocity profile is nearly constant and equal to that of the inlet velocity. As the boundary layer grows, the flow becomes more parabolic in nature and the centerline (maximum) velocity continues to increase to account for the decreased velocity on the walls of the pipe. This is due to the inherent no-slip condition. We also note that the numerical, fully developed velocity profile does not exactly match that of the proposed exact solution. This can be due to several things, including the fact that our numerical tolerance may not have been set low enough to ensure complete convergence of the solution, or the fact that our calculated pressure drop does not accurately represent what is present in the actual system. Overall, we are satisfied with the results shown here and have verfied the nature of the velocity profile for channel, pressure-driven flow.

2.2 Volume Flow Rate

In this section, we will calculate the volume flow rate, Q in the fully developed region using our numerical results and compare this value to that of the exact solution, given by Equation 1. First, the numerical volume flow rate was calculated by taking the average velocity of the flow at the very end of the pipe (where it is fully developed) and multiplying it by the cross-sectional area. Namely,

$$Q_{avg} = v_{avg} \cdot A \tag{4}$$

where the average velocity was calculated in Microsoft Excel as:

$$v_{avg} = 6.10 \cdot 10^{-3}$$

and the cross-sectional area of the pipe is given by:

$$A = \frac{\pi}{4} D^2 = \frac{\pi}{4}(0.01)^2 = 7.854 \cdot 10^{-5}$$

Then using the numerical results, the volume flow rate is given by:

$$Q_{avg} = (6.10 \cdot 10^{-3})(7.854 \cdot 10^{-5}) = 4.79 \cdot 10^{-7} \tag{5}$$

We would like to compare this result against the exact solution, given by Equation 1. First, we need to find dp/dx in the fully developed region. This was done by estimating the entrance length, x_e, for $Re_D = 50$, and then taking the average of dp/dx from this point to the end of the rod. This value was calculated to be:

$$\frac{dp}{dx} = 1.64 \tag{6}$$

Substituing values into Equation 1 yields:

$$Q_{avg} = \frac{\pi R^4}{8\mu} \frac{dp}{dx} = \frac{\pi (0.005)^4}{8(1.0 \cdot 10^{-3})} 1.64 = 4.02 \cdot 10^{-7} \tag{7}$$

The percent error between the numerical results and the exact solution is given by:

$$\%Error = \frac{4.79 \cdot 10^{-7} - 4.02 \cdot 10^{-7}}{4.02 \cdot 10^{-7}} \cdot 100 = 19.2\% \tag{8}$$

This error is quite large, however can be justified by the fact that we are taking average values for velocity and pressure gradients. Furthermore, the axial position from which we are taking these average values (at the end of the rod) was proved to not match that of the exact solution, as shown in Figure 2. Thus, if we were to employ a stricter tolerance on our numerical solution, the volume flow rate obtained from the program might more accurately match that of the exact solution. However, it is still promising that the flow rates given by Equations 5 and 7 are on the same order of magnitude. It shows that we are on the right path, and considering the slight inaccuracy of our model, should be further investigated by improving the convergence tolerance of our solution.

2.3 Entrance Length and it's Relation to Reynold's Number

In this section, we would like to solve for the entrance length, x_e, for the aforementioned numerical results. We would also like to find a relation of x_e to Re_D and compare our results with that in literature. To do so, simulations for 7 different Reynold's Numbers in the range of $Re_D < 1000$ were carried out.

To find the entrance length, it suffices to plot the centerline velocity as a function of axial position and determine where this velocity becomes constant (velocity profile remains constant in the fully developed region). This determination will be made by a guess-and-check method, as it was difficult to fit a trendline to the velocity data. A plot of the centerline velocity vs. axial position for $Re_D = 50$ is given in Figure 3.

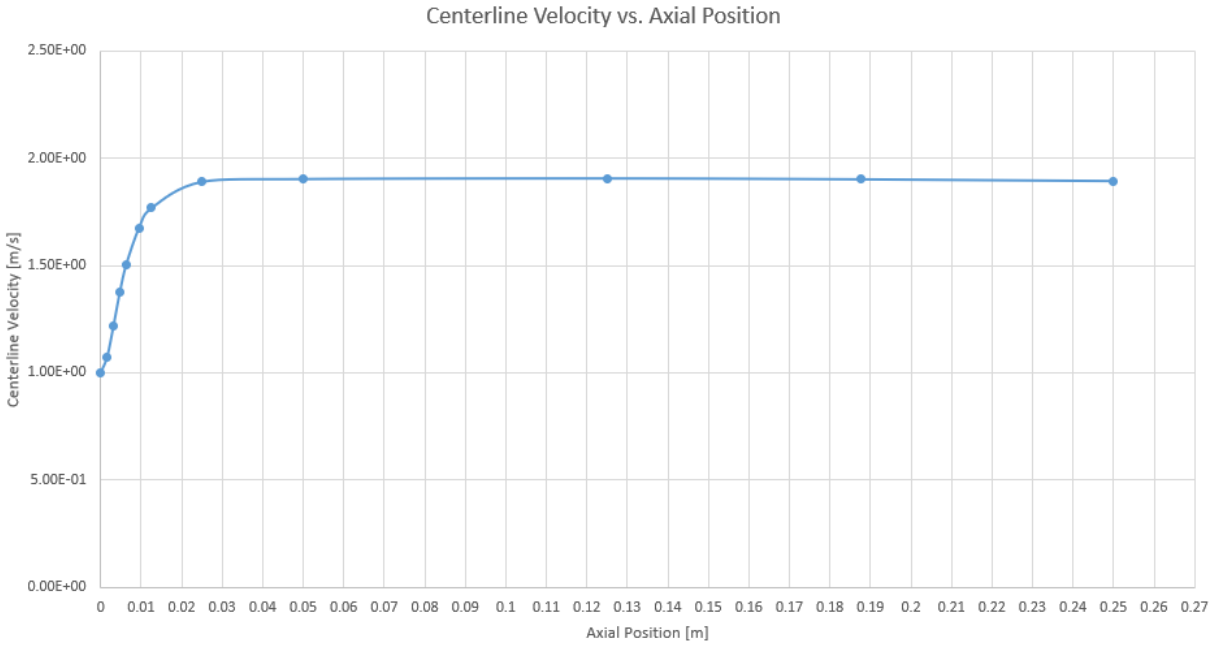

Figure 3: Centerline Velocity vs. Axial Position for$Re_D = 50$

From this plot, we guess that the centerline velocity becomes constant at $x = 0.03$ [m]. Thus, for $Re_D = 50$, the entrance length was calculated as:

$$x_e = 0.03[m] \tag{9}$$

From various sources, it has been determined that entrance length for laminar flow in a pipe should follow the relationship given by:

$$\frac{x_e}{D} = 0.06Re_D \tag{10}$$

For a Reynold's Number of $Re_D = 50$, we see that the result given by Equation 9 directly agrees with that provided in Equation 10. Namely,

$$x_e = (0.06Re_D)D = (0.06)(50)(0.01) = 0.03[m]$$

Thus, we are satisfied with the results for this case. This process was repeated for varying Reynold's numbers within the range $Re_D < 1000$. A plot of the numerically estimated entrance lengths and theoretical entrance lengths vs. varying Reynold's Numbers is shown in Figure 4.

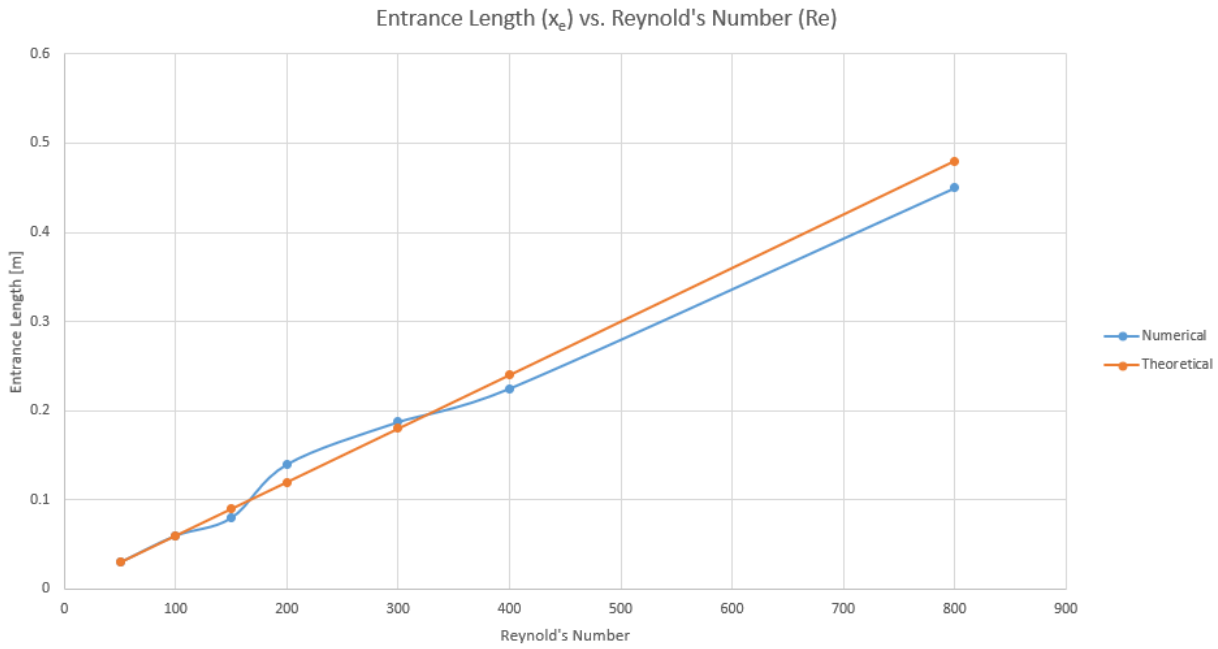

Figure 4: Entrance Length vs. Reynold's Number

From this plot we are able to verify the accuracy of our model in terms of entrance lengths. The estimated numerical entrance lengths almost exactly match those of the theoretical entrance lengths for each Reynold's Number simulation performed. It is obvious from this plot that the entrance length increases linearly with Reynold's Number, as given by Equation 10.

We also note that for $Re_D > 400$, the corresponding entrance length becomes larger than the length of our pipe. I.e., the flow never becomes fully developed. This is not unreasonable, especially considering that our pipe is rather small in length ($L = 0.250$ [m]). Thus, it would be unreasonable to have Reynold's Number above 400 for this specified geometry.

3 Discussion

In this report, we performed several numerical simulations on incompressible, 3-D, viscous laminar channel flow as shown in Figure 1 using ANSYS Fluent. We first noted that this flow contains two distinct regions: the developing region and the fully developed region. Using the Fluent software along with Microsoft Excel, we were able to plot the velocity field in both of these regions, as depicted in Figure 2. We note that near the inlet of the pipe, the flow is still developing, which implies that the velocity field is nearly constant and equal to that of the inlet velocity. As the boundary layer grows and the flow becomes fully developed, the field becomes parabolic in nature, increasing the maximum velocity and enforcing a no-slip condition on the walls of the pipe. The numerical results do not exactly match that of the exact solution, and this could be due to an insufficient convergence tolerance or due to variance in the calculated pressure drop. This is something that should be investigated further if a more detailed analysis was to be performed.

We found that there was a 19.2% difference between the numerical volumetric flow rate and the theoretical volumetric flow rate, as given by Equations 5, 7, and 8. This error can be justified by the fact that we are taking average values for velocity and pressure gradients. Furthermore, the axial position from which we are taking these average values (at the end of the rod) was proved to not match that of the exact solution, as shown in Figure 2.

Perhaps the most successful portion of this report was in verifying the numerical relationship between entrance length and Reynold's Number compared to the theoretical relationship between the two quantities. Several different simulations were performed, each with different Reynold's Number, to get a sense of the relationship between these two quantities. Results for this investigation were depicted in Figure 4. We see that there is very little variation between the numerically estimated entrance length and the theoretical entrance length as given by Equation 10.

Overall, we were able to use ANSYS Fluent to solve for the velocity profile in both the developing and fully developed regions, the numerical and theoretical volumetric flow rate, and were able to compare the numerically estimated entrance length to the theoretical entrance length. The results were representative of those proposed by exact solutions, proving that ANSYS Fluent is a valuable tool in simulating incompressible, 3-D, viscous laminar channel flow.

4 Appendix

4.1 Mesh Generations

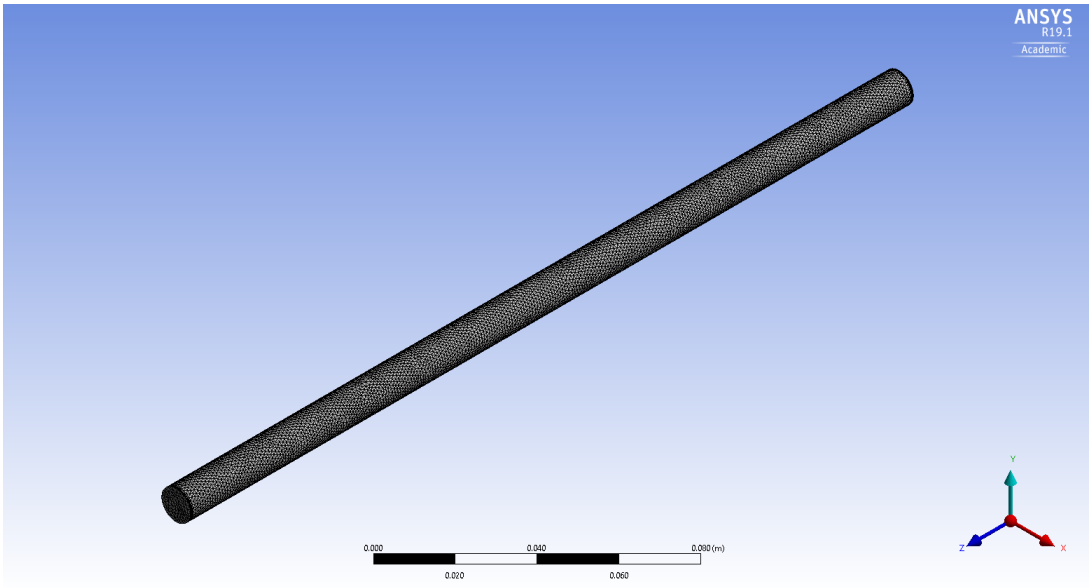

Figure 5: Isometric View of Mesh Generation

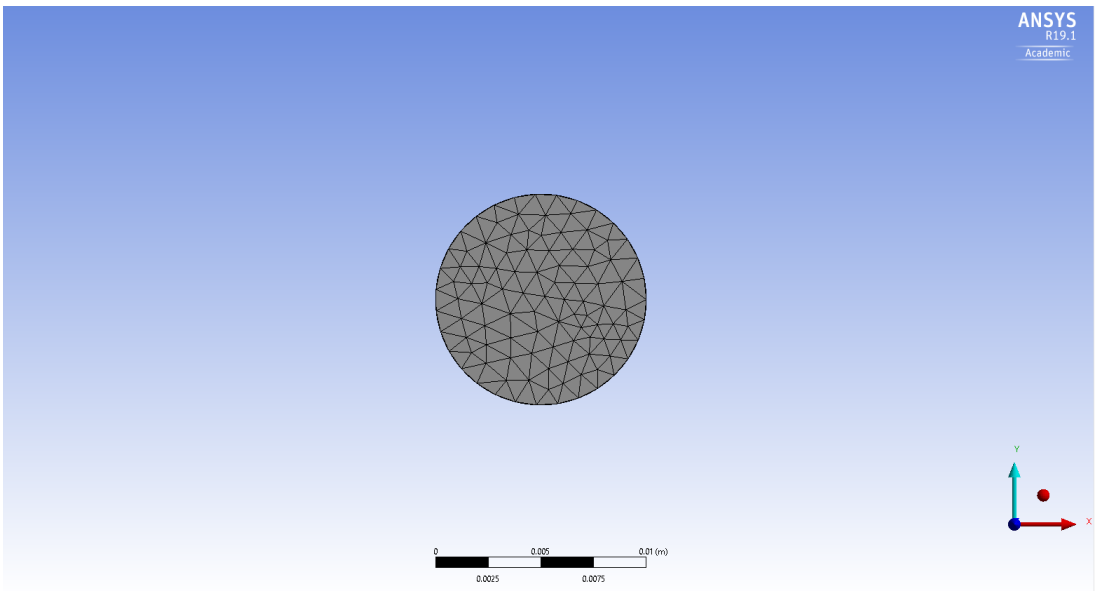

Figure 6: Mesh Generation at the Inlet and Outlet of Pipe

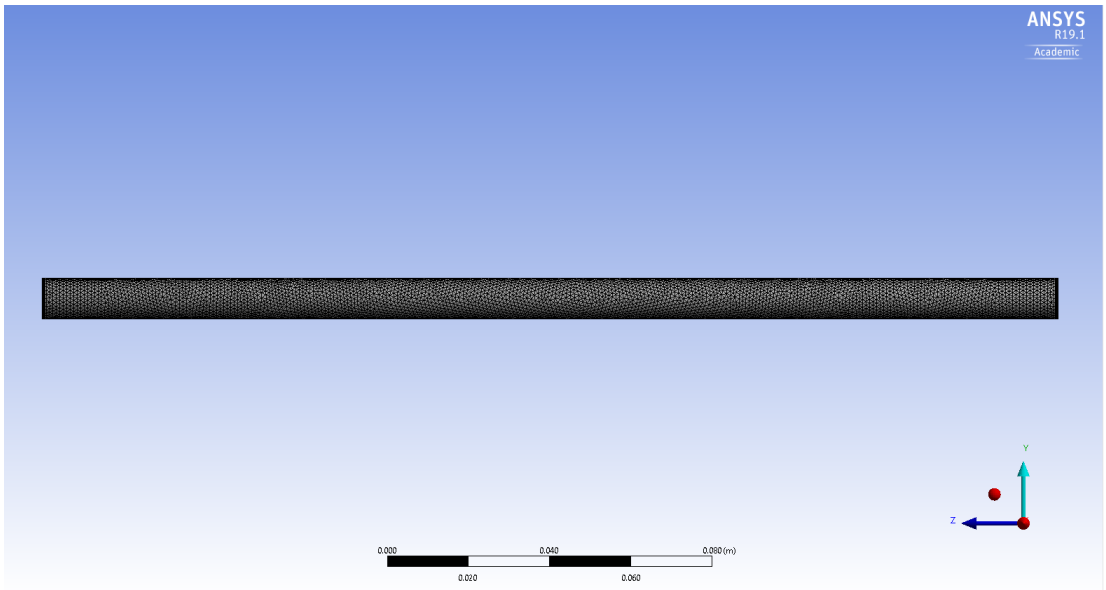

Figure 7: Side View of Mesh Generation at the Wall

4.2 Converging Histories

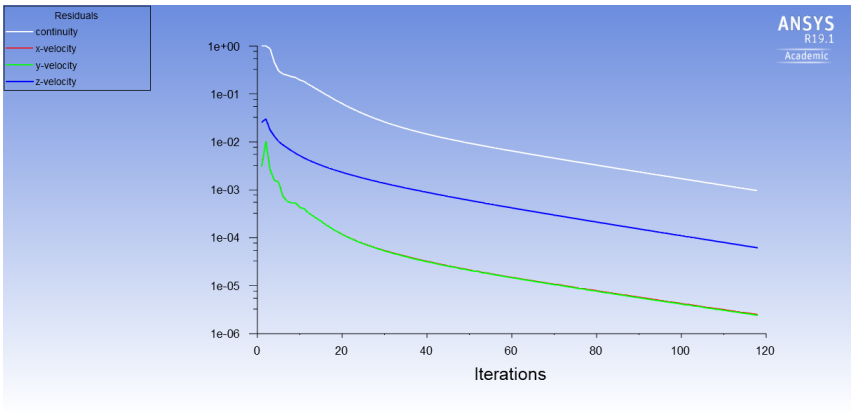

Figure 8: Convergence History for $Re_D = 50$

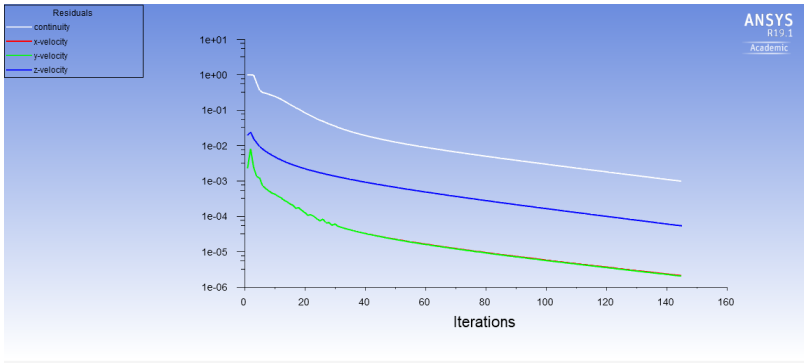

Figure 9: Convergence History for $Re_D = 100$

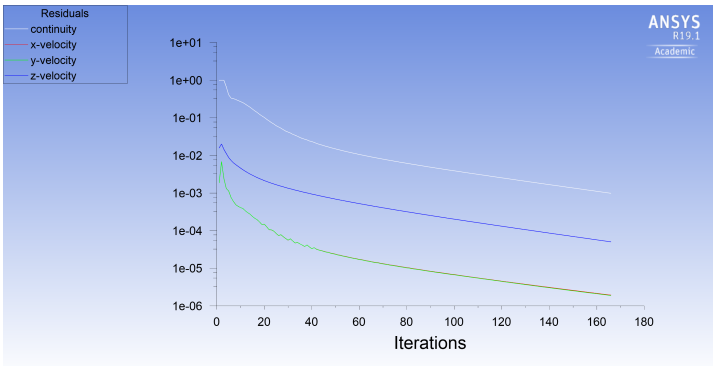

Figure 10: Convergence History for $Re_D = 150$

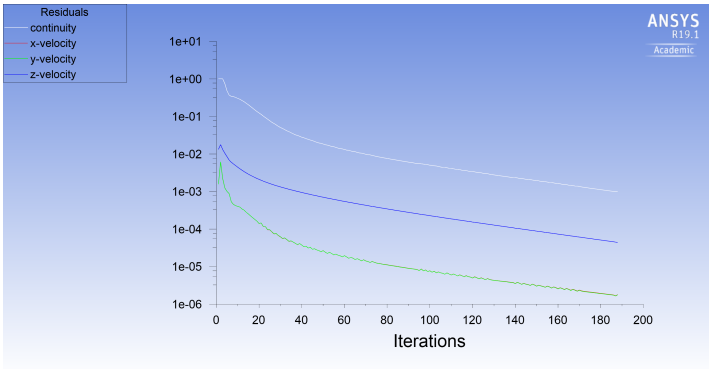

Figure 11: Convergence History for $Re_D = 200$

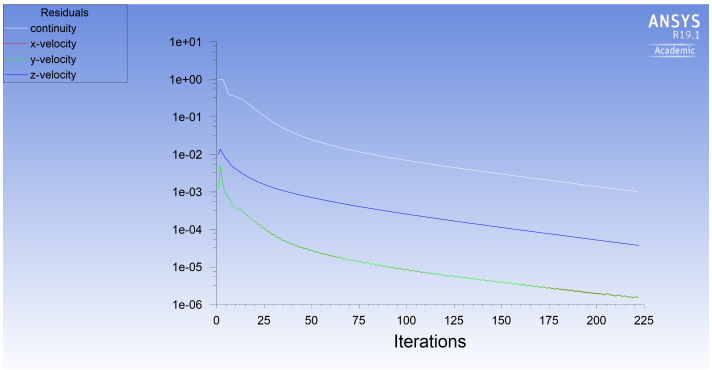

Figure 12: Convergence History for $Re_D = 300$

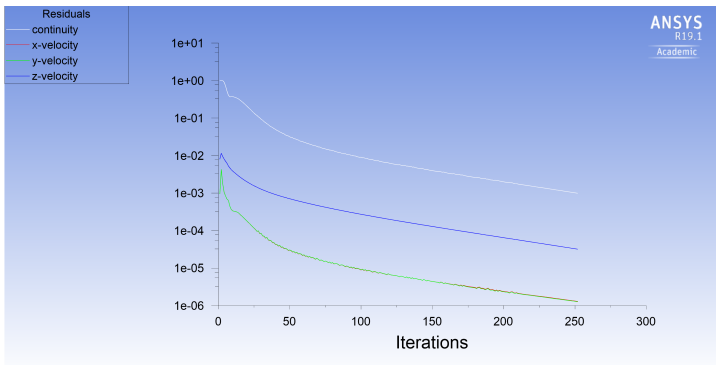

Figure 13: Convergence History for $Re_D = 400$

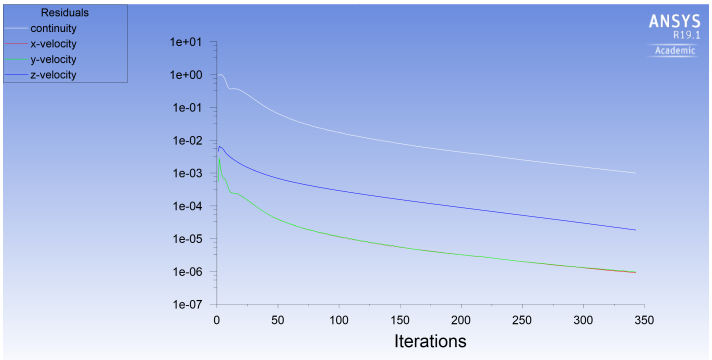

Figure 14: Convergence History for $Re_D = 800$

List of Figures